Cellular/Molecular

In Vivo Identification and Manipulation of the Ca²⁺ Selectivity Filter in the *Drosophila* Transient Receptor Potential Channel

Che H. Liu,[1]* **Tao Wang,**[2]* **Marten Postma,**[1] **Alexander G. Obukhov,**[3] **Craig Montell,**[2] **and Roger C. Hardie**[1]

[1]Department of Physiology Development and Neuroscience, Cambridge University, Cambridge CB2 3DY, United Kingdom, [2]Departments of Biological Chemistry and Neuroscience, Center for Sensory Biology, The Johns Hopkins University School of Medicine, Baltimore, Maryland 21205, and [3]Department of Cellular and Integrative Physiology, Indiana University School of Medicine, Indianapolis, Indianapolis 46202

Null mutations in the *transient receptor potential* (*trp*) gene eliminate the major, Ca²⁺-selective component of the light-sensitive conductance in *Drosophila* photoreceptors. Although it is the prototypical member of the TRP ion channel superfamily, conclusive evidence that TRP is a pore-forming channel subunit *in vivo* is lacking. We show here that mutating a specific acidic residue (Asp^{621}) in the putative pore virtually eliminated Ca²⁺ permeation *in vivo* and altered other biophysical properties of the native TRP conductance. The results identify Asp^{621} as a critical residue of the TRP Ca²⁺ selectivity filter, provide the first rigorous demonstration that a TRP protein is a pore-forming subunit in any native system, and point to the likely location of the pore in mammalian canonical TRP channels. The specific elimination of Ca²⁺ permeation in TRP also provided a unique opportunity to address the roles of Ca²⁺ influx *in vivo*. We found that Asp^{621} mutations profoundly affected several key aspects of the light response and caused light-dependent retinal degeneration.

Key words: photoreceptor; pore; calcium channel; permeability; retinal degeneration; TRP channels; TRPC

Introduction

Belonging to the wider superfamily of voltage-gated channels (for review, see Yu et al., 2005), transient receptor potential (TRP) channels were first identified in *Drosophila* photoreceptors, in which they are believed to mediate the light-induced current (LIC), activated downstream of phospholipase C (PLC). *Drosophila trp* was originally isolated as a mutant, in which the light response decayed to baseline during prolonged illumination (Cosens and Manning, 1969; Minke et al., 1975). The gene was later cloned and found to encode a novel protein with multiple transmembrane (TM) segments reminiscent of cation channels known at the time (Montell and Rubin, 1989). Hardie and Minke (1992) subsequently demonstrated that the Ca²⁺ selectivity of the LIC was profoundly reduced in *trp* mutants and proposed that *trp* encoded a Ca²⁺-selective channel responsible for the major component of the LIC. At the same time Phillips et al. (1992) reported a second gene (*trp*-like, or *trpl*) encoding a protein with 40% identity to TRP, which is now believed to be responsible for the residual LIC in *trp* (Niemeyer et al., 1996; Reuss et al., 1997). In the meantime, numerous TRP homologs have also been identified in vertebrates (Wes et al., 1995; Zhu et al.,

1995), spawning the TRP superfamily with its seven subfamilies. Of these, *Drosophila* TRP and TRPL belong to and define the canonical TRP (TRPC) subfamily, which are all activated downstream of PLC (for review, see Montell, 2005; Ramsey et al., 2006).

Although the *trp* gene is required for the major component of the LIC (Hardie and Minke, 1992), conclusive evidence that it represents a pore-forming subunit *in vivo* is lacking. *Drosophila* TRP has been expressed heterologously, resulting in the appearance of Ca²⁺ and cation-permeable ion channels (Vaca et al., 1994; Xu et al., 1997); however, their biophysical properties showed significant differences from the native conductance. More generally, unambiguous identification of a pore-forming subunit of an ion channel requires the demonstration that mutations in the pore region result in corresponding changes in permeation properties. Although this has been achieved for members of the TRP vanilloid receptor (TRPV) and TRP melastatin (TRPM) subfamilies in heterologous expression studies (Nilius et al., 2001; Voets et al., 2002; Owsianik et al., 2006), in no case has such a demonstration of channel identity been achieved for any TRP channel *in vivo*. Indeed, the selectivity filter has yet to be identified in any of the TRPC subfamily, although mutations in acidic residues lying outside the predicted pore region have been reported to alter the ionic selectivity of heterologously expressed TRPC1 and TRPC5 channels (Jung et al., 2003; Liu et al., 2003).

In the present study, we identified a specific acidic residue (Asp^{621}), which is required for the high Ca²⁺ permeability of the native TRP-dependent current. The results identify the selectivity filter in *Drosophila* TRP and provide an unequivocal demonstra-

tion that TRP is a pore-forming channel subunit *in vivo*. As well as eliminating Ca^{2+} permeation, mutations in Asp^{621} resulted in dramatic changes to the LIC and caused retinal degeneration, thereby providing a direct demonstration of the profound functional role of Ca^{2+} influx in many aspects of phototransduction and cell survival.

Materials and Methods

Flies. Unless otherwise stated, white-eyed (*cn,bw*) *Drosophila melanogaster* were raised in the dark at 25°C. To generate the *trp* transgenes, we used the pHFK–*trp* construct, which spans a 6480 nt *trp* genomic region shown previously to fully rescue the *trp* mutant phenotype (Montell et al., 1985; Li and Montell, 2000). The *trp*^{D621G}, *trp*^{D626G}, *trp*^{D621N}, and *trp*^{D621E} mutations were introduced using the QuickChange method (Stratagene, La Jolla, CA), and the mutant *trp* genomic fragments were subsequently subcloned into the *Not*I site of pCaspeR4. The constructs were injected into *w*^{1118} embryos, and transformants were identified on the basis of eye color. Transgenic lines with third chromosome insertions were selected and, unless otherwise stated, recombined into a *cn,bw*, *trpl*^{302};*trp*^{P343} background (Niemeyer et al., 1996; Wang et al., 2005), so that they were the only light-sensitive channel expressed. Control measurements of wild-type (WT) TRP channel activity were performed in *trpl*^{302} flies and also in *trpl*^{302};*trp*^{P343} flies expressing a wild-type TRP transgene. For *in vivo* measurements of phosphatidylinositol-4, 5-bisphosphate (PIP$_2$) hydrolysis, we used *trpl*^{302};*trp*^{P343} flies expressing the appropriate *trp* transgene and also the PIP$_2$-sensitive Kir2.1^{R228Q} channel as a biosensor under control of the *Rh1* promoter as described previously (Hardie et al., 2001, 2004). The R228Q point mutation reduces the effective affinity of the Kir2.1 channel for PIP$_2$ approximately fivefold, providing a near-linear relationship between PIP$_2$ concentration and K$^+$ current (Hardie et al., 2004).

Whole-cell recordings. Dissociated ommatidia were prepared as described previously from recently eclosed adult flies (Hardie, 1991; Hardie et al., 2001) and transferred to the bottom of a recording chamber on an inverted Nikon (Tokyo, Japan) Diaphot microscope. The standard bath was composed of the following (in mM): 120 NaCl, 5 KCl, 10 *N*-Tris-(hydroxymethyl)-methyl-2-amino-ethanesulphonic acid (TES), 4 MgCl$_2$, 1.5 CaCl$_2$, 25 proline, and 5 alanine. For bi-ionic reversal potential (E_{rev}) measurements, solutions contained 130 mM NaCl, 130 mM *N*-methyl-D-glucamine Cl (NMDG), 10 mM CaCl$_2$, or 10 mM MgCl$_2$ (for divalent ions, 130 mM NMDG was also included). The solutions were applied by broad-mouthed (~10 μm) puffer pipette positioned close to the cells as described previously (Hardie and Mojet, 1995). For measurements of Kir2.1 channel activity, the extracellular solution contained (in mM) 110 NaCl, 10 KCl, 4 CsCl, 1.5 CaCl$_2$, and 4 MgCl$_2$, and measurements were made at a holding potential of −84 mV as described previously (Hardie et al., 2004). Also included in all bath solutions were 10 mM TES, 25 mM proline, and 5 mM alanine. The standard intracellular solution was as follows (in mM): 140 K-gluconate, 10 TES, 4 MgATP, 2 MgCl$_2$, 1 nicotinamide-adenine dinucleotide (NAD), and 0.4 Na GTP. For reversal potential measurements, the following was used (in mM): 130 Cs-gluconate, 10 TES, 3 MgATP, 1 K$_2$ATP, 1 NAD, and 0.4 Na GTP. The pH of all solutions was adjusted to 7.15. All chemicals were obtained from Sigma (Poole, UK).

Whole-cell voltage-clamp recordings were made using electrodes of resistance ~10–15 MΩ, and series resistance values were generally below 25 MΩ and were routinely compensated to >80%. Maximum series resistance errors for E_{rev} measurements were estimated at <2 mV. A correction was made for the measured junction potential (−10 mV). Data were collected and analyzed using an Axopatch 200 amplifier and pClamp 9 software (Molecular Devices, Palo Alto, CA). Cells were stimulated via one of two green light-emitting diodes (LEDs), with maximum intensity of ~3 × 10^5 and 10^8 effectively absorbed photons per second per photoreceptor, respectively. Relative intensities were calibrated using a linear photodiode and converted to absolute intensities in terms of effectively absorbed photons by counting quantum bumps at low intensities in wild-type flies (Henderson et al., 2000).

Immunolocalizations and Western blots. For immunolocalization ex-

periments, adult fly heads were hemisected, fixed in paraformaldehyde, and embedded in LR White. Cross sections (0.5 μm) of compound eyes were obtained from the distal region of the retina, which included the R7 cells. The sections were stained with primary rabbit anti-TRP antibody (1:200) and secondary goat anti-rabbit IgG (Alexa Fluor 488, 1:200; Invitrogen, Carlsbad, CA).

To perform the Western blots, fly heads were homogenized in SDS sample buffer with a Pellet Pestle (Kimble-Kontes, Vineland, NJ). The proteins were fractionated by SDS-PAGE and transferred to Immobilon-P transfer membranes (Millipore, Bedford, MA) in Tris–glycine buffer. The blots were probed with rabbit antibodies [α-TRP, α-INAD (inactivation no afterpotential D), α-G$_q$] or mouse α-Rh1 and then subsequently with α-rabbit IgG peroxidase conjugate (Sigma) or anti-mouse IgG peroxidase conjugate (Sigma). The signals were detected using ECL reagents (Amersham Biosciences, Little Chalfont, UK).

Retinal degeneration. The time course of retinal degeneration was followed by monitoring the integrity of the retina using the presence or absence of the deep pseudopupil (DPP) in white-eyed (*cn,bw*) flies, observed under a stereomicroscope with oblique illumination. Flies were reared in either the dark or a 12 h light/dark cycle in a chamber illuminated by white LEDs (average effective luminance, 100 cd/m^2). Flies were scored as having normal DPP (1.0), a weakly visible DPP (0.5), or no visible DPP (0). A normalized degeneration index was generated from cohorts of newly eclosed flies ($n \geq 15$ for each condition), inspected daily. Degeneration was confirmed by transmission electron microscopy (EM) at representative time points. Flies were prepared and sectioned for EM as described previously (Raghu et al., 2000).

Results

Generation of putative pore mutants

Although TRPL has the properties of a nonselective cation channel with moderate permeability for Ca^{2+} (P$_{\text{Ca}}$:P$_{\text{Cs}}$ ≈ 4:1), the TRP-dependent current (i.e., that eliminated by the *trp* mutation and isolated in the *trpl* mutant) is highly Ca^{2+} selective (P$_{\text{Ca}}$:P$_{\text{Cs}}$ ≈100:1) (Reuss et al., 1997). In several other Ca^{2+}-selective channels, including voltage-gated Ca^{2+} channels (Yang et al., 1993), cyclic nucleotide-gated channels (Eismann et al., 1994), and the Ca^{2+}-selective TRPV5 and TRPV6 channels (Nilius et al., 2001), Ca^{2+} selectivity is believed to be conferred by a ring of four acidic residues within the pore, which coordinate a binding site for divalent ions. We therefore compared the sequences of TRP and TRPL in the putative pore region and sought acidic residues that were unique to TRP. Over the ~30 amino acids immediately N-terminal to the sixth transmembrane helix (TM6), the TRP and TRPL sequences show a high degree of identity (78%). However, close to the expected vicinity of the pore, there is one aspartate (Asp^{621}) in TRP, which is substituted for glycine in TRPL, and a second aspartate (Asp^{626}), which is conservatively substituted for another acidic residue (glutamic acid) in TRPL. The only other acidic residue in the vicinity of the putative pore of TRP (Glu^{607}) is conserved in TRPL (Fig. 1*A*).

To test whether either of these acidic residues was responsible for the high Ca^{2+} selectivity of TRP, we generated mutant genomic transgenes encoding TRP isoforms in which the aspartate residues were neutralized to glycine (*trp*^{D621G} and *trp*^{D626G}). Flies stably expressing these transgenes were generated by germline transformation. Unless otherwise stated, the mutant TRP channels were expressed in a *trpl*^{302};*trp*^{P343} double null mutant background, so that they were the only light-sensitive channels expressed in the photoreceptors. Western blot analysis confirmed that the mutant TRP proteins were stably expressed, although the levels of TRP^{D626G} were lower than in wild type (Fig. 1*B*). Immunostaining revealed that TRP^{D621G} and TRP^{D626G} were correctly targeted to the microvillar portion of the photoreceptor cells, i.e., the rhabdomeres (Fig. 1*C*). Other major components of the

transduction cascade, including G_q, Rh, PLC [NORPA (no receptor potential A)], and the PDZ (postsynaptic density-95/Discs large/zona occludens-1) domain scaffolding protein (INAD), were expressed at normal levels in both mutants (supplemental Fig. S1, available at www.jneurosci.org as supplemental material).

Ionic selectivities

We determined ionic selectivities by measuring the E_{rev} of the LIC from whole-cell voltage-clamped photoreceptors. The intracellular solution contained Cs^+ (130 mM) as the only cation, apart from trace amounts of unchelated Mg^{2+}, K^+, and Na^+ in nucleotide salts (ATP/GTP), required to sustain the operation of the phototransduction cascade.

With the normal physiological bath solution (in mM: 120 Na^+, 5 K^+, 1.5 Ca^{2+}, and 4 Mg^{2+}), E_{rev} for the wild-type TRP channel isolated in *trpl* mutants (or *trpl; trp* expressing a wild-type *trp* transgene) was +19.2 ± 2.2 mV (mean ± SD; n = 34). As reported previously (Reuss et al., 1997), this rather positive value reflects both a significant selectivity for Na^+ over Cs^+, which is diagnostic of high field strength sites (Eisenmann series ≥ V), and also the significant permeation of Ca^{2+} and Mg^{2+} ions in the bath solution. Accordingly, under bi-ionic conditions, with 130 mM Na^+ as the only permeable extracellular cation, $P_{Na}:P_{Cs}$ was estimated as 1.3:1 (E_{rev} of +6 mV), whereas with 10 mM extracellular Ca^{2+} or Mg^{2+}, E_{rev} values of +35 and +10 mV, respectively, indicated permeability ratios of ~60:1 ($P_{Ca}:P_{Cs}$) and 16:1 ($P_{Mg}:P_{Cs}$) (Fig. 2, Table 1). E_{rev} in bath containing 130 mM NMDG (the "impermeant cation" in the divalent cation solutions) was −75 mV, indicating a small residual permeability for this large organic cation.

To characterize the mutagenized TRP channels in the absence of TRPL, we obtained E_{rev} data from *trpl;trp* flies expressing the transgenic TRP^{D621G} or TRP^{D626G} channels. E_{rev} values determined under both control and bi-ionic conditions in *trp*^{D626G} were very similar (within ~5–10 mV) to those recorded in control (*trpl*) flies expressing wild-type TRP channels. However, we found large shifts in E_{rev} in *trp*^{D621G}, indicating profoundly altered ionic selectivity profiles. With Na^+ as the only external cation, a ~15 mV negative shift in E_{rev} to −8 mV revealed that permeability for Cs^+ was now greater than for Na^+, indicating a shift toward a lower field strength site (Eisenmann series I–IV). Even more strikingly, the same single amino acid substitution induced huge (~100 mV) negative shifts in E_{rev} for divalent ions, to −65 mV for 10 mM Ca^{2+} and −73 mV for Mg^{2+}. For Mg^{2+}, this was indistinguishable from E_{rev} determined in the presence of NMDG alone (−76 mV), indicating that the channels were essentially impermeable for Mg^{2+}, whereas for Ca^{2+}, E_{rev} was slightly more positive than for NMDG, indicating a small residual permeability for Ca^{2+} ($P_{Ca}:P_{Cs}$ < 0.2). Compared with the wild-type channel, however, the reduction in relative permeability for divalent ions was several hundred-fold, indicating that this single amino acid substitution had converted a primarily Ca^{2+}-selective channel into one that permeates almost exclusively monovalent cations.

Titrating the charge on Asp⁶²¹ reduces relative permeability for both Ca²⁺ and Na⁺

If Asp⁶²¹ does indeed represent a key pore-lining residue responsible for Ca^{2+} selectivity, then one would predict that manipulating the charge and/or side chain length of this residue would result in additional systematic changes in permeation properties. We therefore generated flies in which Asp⁶²¹ was mutated to a polar residue, asparagine (*trp*^{D621N}), and to glutamic acid (*trp*^{D621E}), another acidic residue with a longer side chain and a weaker p_K. The concentrations of the TRP protein levels in both of these transgenic lines were at least as high as in wild-type flies (Fig. 1*B*).
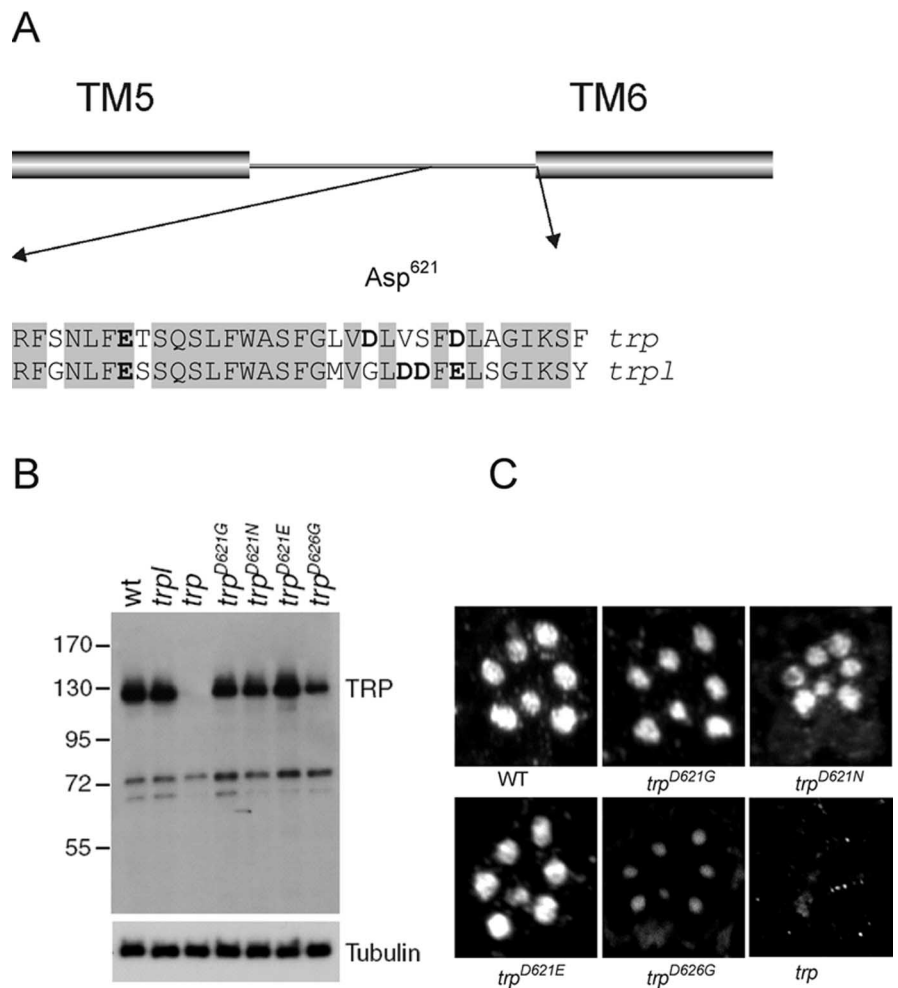

Figure 1. Generation and expression of mutations in acidic residues in putative selectivity filter. ***A***, Alignment of TRP and TRPL sequences in the vicinity of the putative pore region, which by analogy to other channels would be expected to be located toward the end of the region linking TM5 and TM6. Acidic residues are indicated in bold. A total of 78% of residues are identical in this region (shaded). Asp⁶²¹ and Asp⁶²⁶ are the only acidic residues unique to TRP sequence. ***B***, Western blot showing TRP protein levels in *trpl*, wild-type, *trp*, and the four transgenic lines used in this study: *trp*^{D621G}, *trp*^{D621N}, *trp*^{D621E}, and *trp*^{D626G}. The blot was also probed with α-β-tubulin antibodies to provide a loading control. ***C***, Immunofluorescent localization of mutant TRP isoforms in semithin LR White sections stained with α-TRP antibodies. Each image shows the pattern of rhabdomeres in one ommatidium. All TRP isoforms were correctly localized, although the TRP^{D626G} signal was weaker because of the lower level of expression. No staining above background was seen in the negative control (*trp*), which was the null allele *trp*^{343} (Wang et al., 2005).
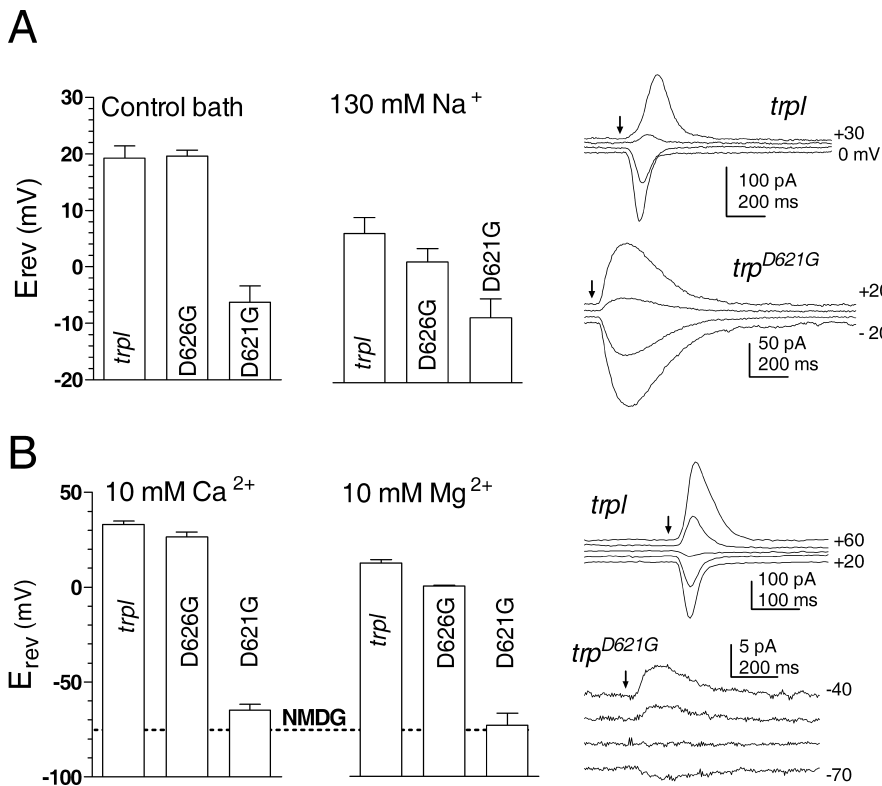
Figure 2. Reversal potential measurements in putative pore mutants. Reversal potentials (E_{rev}, mean $\pm$ SD) measured from responses to brief flashes at different holding potentials in 10 mV steps (sample traces shown on the right). **A**, In control bath (in mM: 1.5 Ca²⁺, 4 Mg²⁺, 120 Na⁺, and 5 K⁺) ($n = 6$–34 cells) and under bi-ionic conditions with only 130 mM NaCl in the bath ($n = 4$–6). **B**, Under bi-ionic conditions with 10 mM Ca²⁺ ($n = 4$–9) or 10 mM Mg²⁺ ($n = 3$–7), using 130 mM NMDG as impermeant cation in bath. E_{rev} values in trp^{D626G} were within ~5–10 mV of control $trpl$ values. In contrast, massive shifts were observed in trp^{D621G}. The dotted line shows the mean E_{rev} for 130 mM NMDG alone (-76 mV), which was indistinguishable from E_{rev} recorded in 10 mM Mg²⁺ but slightly more negative than that in 10 mM Ca²⁺. In all cases, the intracellular electrode contained 130 mM Cs gluconate. The *trp* transgenes were expressed on a $trpl^{302};trp^{P343}$ background.

Table 1. Permeability ratios measured under bi-ionic conditions in *trpl* (to isolate the wild-type TRP channel) and in flies expressing different *trp* transgenes (all expressed on *trpl;trp* double-mutant background)

	P_{Ca}:P_{Cs}	P_{Mg}:P_{Cs}	P_{Na}:P_{Cs}	P_{NMDG}:P_{Cs}
WT (trpl)	56.9	15.8	1.30	0.04
trp^{D626G}	35.2	7.4	1.06	n.d.
trp^{D621E}	23.0	2.9	1.17	0.02
trp^{D621N}	~0.2	0	0.99	0.02
trp^{D621G}	~0.1	0	0.70	0.04
trp^{D621N}/+	15.5	n.d.	n.d.	n.d.
trp^{D621G}/+	4.3	n.d.	n.d.	n.d.

n.d., Not determined. Internal solution contained 130 mM Cs$_{in}$. External solutions contained 10 mM Ca²⁺, 10 mM Mg²⁺, 130 mM Na⁺, or 130 mM NMDG (divalent cation solutions also contained 130 mM NMDG). Permeability ratios were derived from E_{rev} measurements according to the following:

$$\frac{P_X}{P_{Cs}} = \exp(E_{rev}F/RT), \qquad (1)$$

in which X is the monovalent cation, and

$$\frac{P_X}{P_{Cs}} = \frac{1}{4}\frac{[Cs^+]_i}{[X^{2+}]_e}\exp(E_{rev}F/RT)(\exp(E_{rev}F/RT) + 1), \qquad (2)$$

in which X is the divalent cation.

With the polar but uncharged asparagine substitution (trp^{D621N}), both Mg²⁺ and Ca²⁺ selectivities were again profoundly reduced; however, the residual Ca²⁺ permeability was marginally but significantly higher ($p < 0.05$). The relative permeability for Na⁺ was also substantially reduced compared with wild type, but again significantly less so than in trp^{D621G} (Fig. 3A).

In contrast, when Asp[621] was substituted for glutamic acid (trp^{D621E}), substantial Ca²⁺ permeation was maintained. Nevertheless, even with this more conservative substitution, the channels still showed significant changes to their ionic selectivity profile. E_{rev} in 10 mM Ca²⁺ was negatively shifted by 12 mV, indicating an approximately threefold reduction in P_{Ca}: P_{Cs} to only ~20:1, whereas there was also a significant decrease in P_{Na}:P_{Cs} to 1.17.

In addition, we generated heteroallelic flies, expressing one copy of the wild-type *trp* gene and one copy of trp^{D621G} or trp^{D621N}, in which the majority of the ion channels should be heteromultimers containing both wild-type TRP and mutant TRP$^{D621G/N}$ subunits. The LIC in photoreceptors from these flies had intermediate reversal potentials, indicating that such heteromultimers also have greatly altered ionic selectivity. E_{rev} for the heteroallelic trp^{D621G}/+ flies were significantly more negative than for trp^{D621N}/+, particularly for bi-ionic conditions with Ca²⁺ as the sole extracellular cation. Close examination of the traces of recordings from trp^{D621G}/+ or trp^{D621N}/+ photoreceptors also revealed that responses near reversal potential were clearly biphasic, indicating contributions of channels with different E_{rev} (Fig. 3A). Presumably, these represented heteromultimers with different subunit stoichiometry (i.e., 2:2 and 1:3). The earlier phases of these biphasic currents were always inward, indicating that the channels with higher Ca²⁺ permeability were more rapidly activated, consistent with previous studies indicating that TRP channel activity is facilitated and accelerated by Ca²⁺ influx (Hardie, 1991, 1995). Formally, we cannot exclude the possibility that the conductances responsible for these biphasic reversal potentials represent the independent contribution of pure WT and pure mutant homotetramers. However, it is difficult to envisage a mechanism that would prevent otherwise identical subunits, expressed under control of the same promoter, from being assembled as heteromultimers.

In summary, for both Ca²⁺ and Na⁺ permeation, there was a clear, continuous and systematic trend of decreasing permeability, which follows the decreasing charge on this residue: Asp > TRP^{D621E} > TRP^{D621N}/+ > TRP^{D621G}/+ > TRP^{D621N} > TRP^{D621G} (Fig. 3). The fact that neutralizing or otherwise manipulating Asp[621], but not the other acidic residue in the putative pore region (Asp[626]), had such dramatic and charge-dependent effects on Ca²⁺ permeability and smaller but still highly significant effects on the permeation of monovalent ions indicates that Asp[621] is a pore-lining residue with a key role in conferring the high Ca²⁺ selectivity of the wild-type TRP channel.

Remodeling Asp[621] influences pore diameter and single-channel conductance

Interestingly, E_{rev} measured in the presence of NMDG alone was ~15 mV more negative in both trp^{D621E} and trp^{D621N} (but not trp^{D621G}) than for the wild-type channel, suggesting that these
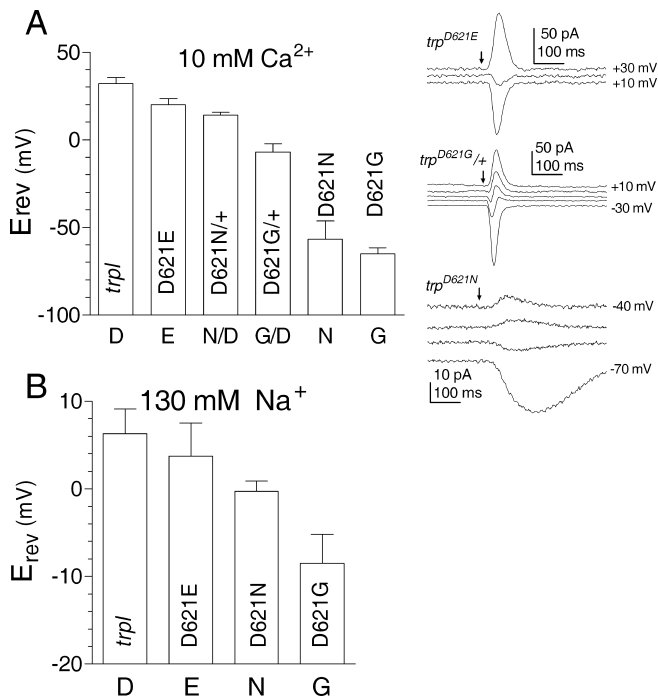
Figure 3. ***A***, ***B***, Bi-ionic reversal potentials. E_{rev} recorded in 10 mM Ca²⁺ (***A***) ($n = 4$–9 cells) and 130 mM Na⁺ (***B***) ($n = 3$–4), in *trp*[302];*trp*[P343] flies expressing *trp* transgenes with the indicated substitutions of Asp [621] (glutamic acid, *trp*[D621E]; asparagine, *trp*[D621N]; and glycine, *trp*[D621G]). For 10 mM Ca²⁺, values are also shown for heteroallelic flies expressing one copy of the *trp*[D621N] or *trp*[D621G] transgenes and one copy of wild-type *trp* (D621N/+, D621G/+). Representative traces were all recorded in 10 mM Ca²⁺. Results, which are plotted in order of decreasing charge on Asp [621], show a continuous gradation in both relative Ca²⁺ and Na⁺ permeability as the charge on Asp [621] is reduced. D, E, N/D, G/D, N, and G indicate residues.

mutations may also have reduced the absolute pore diameter To explore this more systematically, we measured relative permeability for a number of organic cations ranging in size from 4.6 Å (dimethylammonium) to 6.8. Å (NMDG). The results (Fig. 4) confirmed striking and significant differences shifts in E_{rev}, with up to ~40 mV negative shifts in E_{rev} in *trp*[D621E] and smaller, although still significant, shifts in *trp*[D621N] and *trp*[D621G] photoreceptors. In principle, the permeability ratios (P_X:P_{Cs}) derived from these data (using Eq. 1 in Table 1) can be used to estimate the effective diameter of pore, if this is assumed to act as a simple molecular sieve. In this case, permeability should decrease with increasing cation diameter according to some form of excluded volume equation (Dwyer et al., 1980), for example, as follows:

$$P_X:P_{Cs} = k(1 - a/d)^2/a, \tag{3}$$

where d is the pore diameter, and a is the diameter of the cation. Fitting all of the data to this equation suggests the wild-type TRP channel has a diameter of 8.6 Å (Fig. 4*B*, solid curve). However, the data point for dimethylammonium in particular appeared to be poorly fitted, and, if this was omitted from the fit, an estimate of 7.4 Å was obtained (Fig. 4*B*, dotted curve). The data for the three mutants were all reasonably fitted by Equation 3, yielding the estimates of pore diameter shown in the inset to Figure 4*B*. The analysis suggests a conspicuous reduction in pore diameter (to 6.6 Å) in the TRP [D621E] channel, which would be consistent with the extra length (one additional C–C bond) of the glutamate side chain, assuming that this residue occupies the narrowest part of the pore. Estimates of the pore diameter for TRP [D621N] (7.5 Å) and TRP [D621G] (7.8 Å) fell between the two estimates for the WT
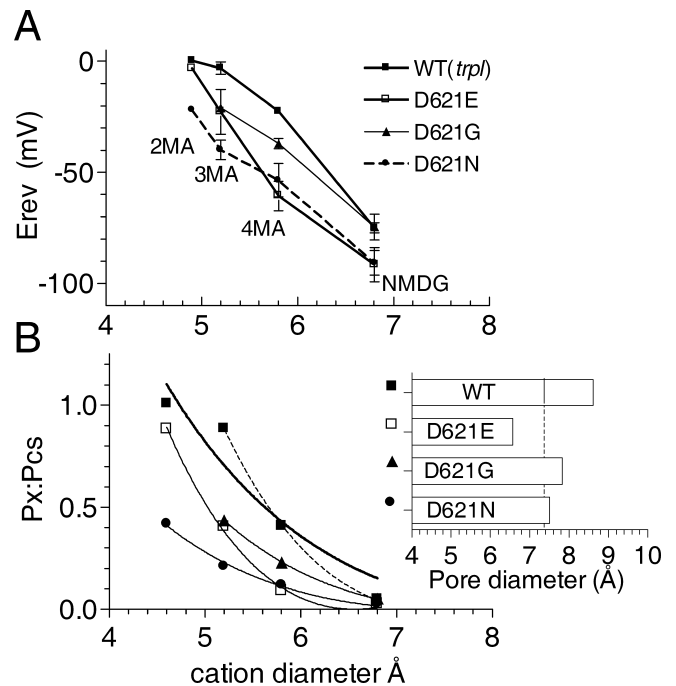

Figure 4. Permeability to organic cations. ***A***, E_{rev} recorded under bi-ionic conditions (130 mM Cs_in) with a series of organic cations of increasing size (all 130 mM), dimethylammonium (2MA), trimethylammonium (3MA), tetramethylammonium (4MA), and NMDG. Mean ± SD; $n = 3$–7 cells per data point. ***B***, Relative permeabilities (P_X:P_{Cs}; Eq. 1 in Table 1) derived from data in ***A***, plotted against cation diameter. The data have been fitted with an excluded volume equation (Eq. 3). On the assumption that relative permeability is determined by size alone, this can be used to derive the effective diameter of the pore. The data for the wild-type channel (WT is *trpl* mutant) have been fitted both with (solid curve) and without (dotted curve) the data point for dimethylammonium (see Results). The inset shows the effective diameter of the pore derived from these fits: the wild-type pore diameter was estimated at 8.6 Å when the dimethylammonium data point was included in the fit but only 7.4 Å when it was excluded (dotted line). The estimated TRP [D621E] pore diameter (6.6 Å) was substantially smaller than either of these estimates, whereas values for TRP [D621N] and TRP [D621G] fell between the two wild-type estimates.

channel, leaving it uncertain as to whether pore diameter was also altered in these mutants. However, the differences in relative permeabilities for several organic cations in both *trp*[D621G] and *trp*[D621N] photoreceptors are an additional clear indication of alterations to the permeation pathway in both TRP [D621N] and TRP [D621G] channels.

Although only one of many factors that can influence single-channel conductance, we also asked whether the changes in effective pore diameter induced by Asp [621] mutations might also be reflected in the single-channel currents. Estimates of single-channel conductance can be derived by steady-state noise analysis of spontaneous channel activity ("rundown current") after metabolic inhibition (Hardie and Minke, 1994; Agam et al., 2000), although the small single-channel conductance, combined with very short open times (~0.5 ms) and the high capacitance (>50 pF) of the photoreceptors (resulting in slow clamp time constants), makes accurate estimates difficult. Under optimal conditions, the wild-type TRP channel (isolated in *trpl*) has been estimated to have a single-channel conductance of ~8 pS (Raghu et al., 2000); however, such values have only been resolved in mutants with greatly reduced microvillar surface area (and hence lower capacitance), and, in normal wild-type or *trpl* photoreceptors, the derived values are typically 2–4 pS (Hardie and Minke, 1994; Reuss et al., 1997).

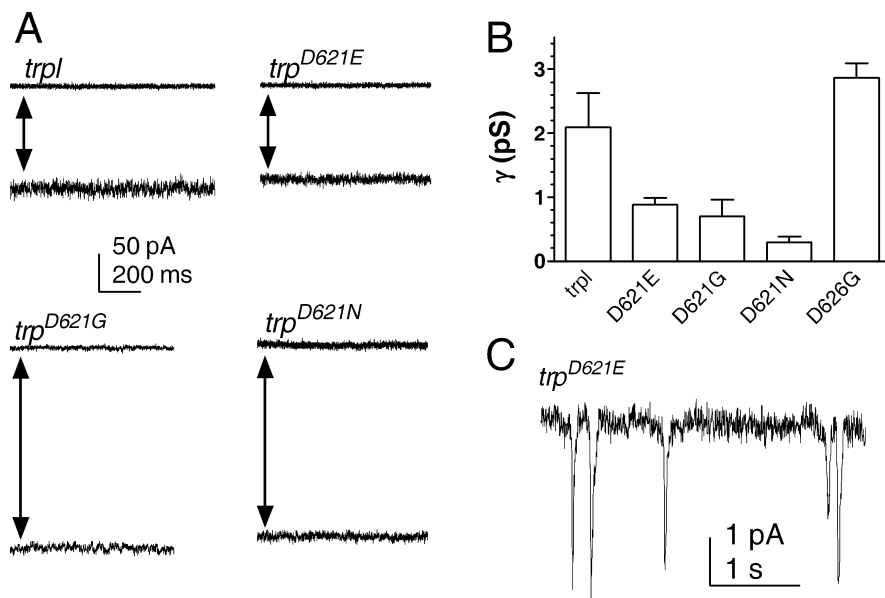After channel activation by the metabolic inhibitor dinitrophenol (DNP) (100 μM), we were able to resolve a low level

Figure 5. Spontaneous channel noise recorded after activation by the metabolic inhibitor DNP (100 μM) (Agam et al., 2000; Hardie et al., 2003). **A**, Each pair of traces shows control noise in the dark (top) before channel activation and steady-state channel noise after activation by DNP. **B**, The underlying single-channel currents were calculated as variance/mean current (after subtracting the dark control values) and converted to effective single-channel conductances (γ) assuming respective measured reversal potentials (mean ± SD; n = 4–5 cells for each genotype). Measurements were made in both series compensated (>80%) and uncompensated mode. For uncompensated cells, a correction was made for the noise lost by filtering by the clamp time constant as described previously (Hardie and Minke, 1994; Reuss et al., 1997). This required knowledge of the frequency characteristics of the channel openings, which were derived by Lorentzian fits to power spectra of the noise. Both approaches yielded similar values. Values for TRP^{D621G} channels were not significantly different from TRP^{D621E} but were significantly (p = 0.03) larger than for TRP^{D621N}. Both TRP^{D621E} and TRP^{D621G} channel conductances were significantly smaller than WT (p = 0.003). **C**, Quantum bumps recorded in response to dim illumination in trp^{D621E}. Mean amplitude (3.7 ± 1.1 pA; n = 4 cells) was ~40% of that recorded in wild-type or trpl flies (9–10 pA) (Henderson et al., 2000). Waveform and duration (half-width of 24 ± 6 ms) were similar to wild-type bumps.

of channel noise in favorable recordings of the steady-state rundown currents (Fig. 5A). After appropriate analysis (see legend to Fig. 5), such recordings yielded effective single-channel conductance estimates of 0.3 pS for TRP^{D621N}, 0.7 pS for TRP^{D621G}, and 0.9 pS for TRP^{D621E}, whereas the wild-type channel (in trpl) recorded under the same conditions yielded values of 2.1 pS, within the range reported previously. Values for TRP^{D621G} and TRP^{D621E} were not significantly different from each other, but both were significantly smaller than the wild-type channel (p < 0.005) and larger than for TRP^{D621N} (p < 0.03). In contrast, the estimated single-channel conductance (2.9 pS) for TRP^{D626G} was similar although apparently slightly larger than the wild-type channel (Fig. 5B).

Asp^{621} mutations influence the block by Mg^{2+} and ruthenium red but not La^{3+}

In common with other highly selective Ca^{2+} channels, monovalent currents mediated by wild-type TRP channels are blocked by extracellular divalent ions. Because of additional actions of Ca^{2+} on components of the transduction cascade, it is only practicable to quantify this block for the case of Mg^{2+}, which was reported previously to block the wild-type LIC in a voltage-dependent manner with an IC$_{50}$ of 280 μM (Hardie and Mojet, 1995). To ask whether the same acidic residue responsible for Ca^{2+} selectivity might also be responsible for divalent ion block, we measured the block of the LIC in the absence of extracellular Ca^{2+} while varying the extracellular Mg^{2+}. In trpl mutants, IC$_{50}$ was estimated at

240 μM, i.e., slightly lower than the value reported previously in wild-type flies expressing both TRP and TRPL channels (Hardie and Mojet, 1995). However, in trp^{D621G}, the IC$_{50}$ was shifted ~10-fold to 2.1 mM (Fig. 6A).

Asp^{621} mutations also resulted in a striking change in the rectification characteristics of the conductance. As reported previously, in physiological solutions, the wild-type TRP channel (in the trpl^{302} mutant) showed a dual inward and outward rectification with a low slope conductance between −10 and +40 mV primarily attributable to a voltage-dependent Mg^{2+} block (Hardie and Mojet, 1995). In marked contrast, in both trp^{D621G} and trp^{D621N}, the slope conductance was high in this region, whereas the overall rectification characteristics were now independent of extracellular divalent ions (data not shown). In both trp^{D621G} and trp^{D621N}, an additional complex double rectification developed below −40 mV and above +100 mV. The basis of this was not further investigated, but the near zero slope conductance between −100 and −30 mV is probably a reflection of intrinsic voltage dependence of the channels revealed in the absence of Ca^{2+} influx (i.e., the expected increase in current attributable to the greater driving force is counteracted by lower open probability). The rectification profile in trp^{D626G} was very similar to that in wild-type (Fig. 6B), whereas in trp^{D621E}, it appeared intermediate between that in trp$^{D621G/N}$ and wild-type (data not shown).

Although these results are consistent with Asp^{621} also representing the binding site responsible for the voltage-dependent block by Mg^{2+}, we cannot exclude the possibility that the site lies deeper within the channel, as reported for TRPC5 (Obukhov and Nowycky, 2005). This is because, unlike the case for the wild-type TRP channel, neither TRP^{D621G} and TRP^{D621N} appear to permeate Mg^{2+}, and hence extracellular Mg^{2+} would no longer have access to sites deeper within the pore or in the inner vestibule.

Many Ca^{2+}-permeable channels, including several TRP channels, are also blocked by the polyvalent cation ruthenium red (RR), and targeted mutagenesis in TRPV1 and TRPV4 has suggested that the same residue responsible for Ca^{2+} selectivity also represents the RR binding site (Garcia-Martinez et al., 2000; Voets et al., 2002). We found that the LIC mediated by both the wild-type TRP channel (isolated in trpl) and TRP^{D626G} was also almost completely (80–90%) blocked by 1 μM RR (Fig. 6C) and completely blocked by 10 μM RR. In contrast, 1 μM RR induced at most only a weak block (<20%) of either TRP^{D621G} or TRP^{D621N} channels, whereas TRP^{D621E} channels showed an intermediate sensitivity. Responses in trp^{D621G} were ~90% blocked by increasing the concentration of RR to 10 μM (n = 3), indicating an ~10-fold reduction in the affinity for this channel blocker.

Finally, another hallmark of the TRP channel that distinguishes it from TRPL channels is its sensitivity to block by low micromolar concentrations of La^{3+}. We therefore asked whether Asp^{621} might also represent the site of action of La^{3+}; however, in

fact, TRP^{D621G} and TRP^{D626N} as well as TRP^{D626G} channels were all blocked to a similar degree (~80–90%) by 1 μM La^{3+} and, like the wild-type channel, completely blocked by 10 μM La^{3+}. This indicates that the La^{3+} binding site includes residues other than Asp^{621} and Asp^{626} (Fig. 6*C*).

Ca²⁺-dependent shaping of the light response

As well as identifying a critical molecular determinant of Ca^{2+} selectivity and providing unequivocal demonstration of the identity of TRP as a pore-forming subunit *in vivo*, the availability of photoreceptors expressing Ca^{2+}-impermeable TRP channels provides a powerful tool allowing the direct and independent *in vivo* testing of many of the proposed functional roles for Ca^{2+} influx via TRP channels in *Drosophila*.

Under normal physiological conditions, phototransduction in fly photoreceptors is regarded as the fastest known G-protein-coupled signaling cascade (for review, see Montell, 1999; Hardie and Raghu, 2001). Ca^{2+} influx via TRP channels has been proposed to be essential for these rapid kinetics, because removing extracellular Ca^{2+} greatly slows down both the rising and falling phases of the response (Hardie, 1991, 1995; Ranganathan et al., 1991). However, such results do not exclude the involvement of extracellular Ca^{2+} binding sites or effects mediated by changes in intracellular Ca^{2+} levels, which accompany changes in extracellular Ca^{2+}. We therefore investigated the effects on phototransduction resulting from virtually eliminating Ca^{2+} influx by neutralizing Asp^{621}.

Indeed, the most immediately obvious phenotype of photoreceptors expressing TRP^{D621G} channels was the ~10-fold slower kinetics of the light response (Fig. 7). Strikingly, the kinetics and amplitude of responses in these transgenic flies no longer showed any significant differences when Ca^{2+}-free solutions were rapidly applied by perfusion with puffer pipettes (Fig. 7*C*,*E*). Furthermore, the waveforms of flash responses recorded in physiological, Ca^{2+}-containing solutions were indistinguishable from those recorded in wild-type or *trpl* flies in the absence of extracellular Ca^{2+} (Fig. 7*D*,*E*). The response kinetics in *trp*^{D621N} flies in Ca^{2+}-containing solutions were similarly slow to *trp*^{D621G} (data not shown); however, in *trp*^{D621E}, in which there was only a modest reduction in Ca^{2+} selectivity, the kinetics of the light response were only slightly slower than those recorded in wild-type flies and similarly sensitive to extracellular Ca^{2+} (Fig. 7*B*,*E*).

Quantum bumps

Ca^{2+}-dependent feedback is believed to be mediated primarily at the level of the quantum bumps, which are the responses to single absorbed photons. Normally, these are ~10 pA in amplitude and
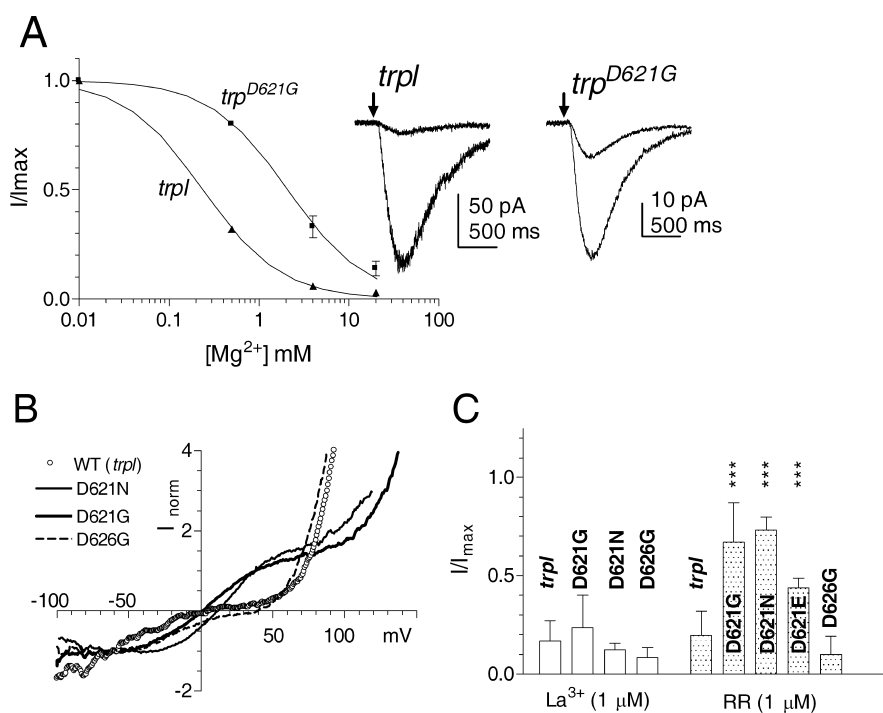

Figure 6. Modification of channel block by Asp ^{621} mutations. *A*, Inhibition of the LIC by extracellular Mg $^{2+}$ in Ca $^{2+}$-free bath (120 mm NaCl, 5 mm KCl, and 0 Ca $^{2+}$). The light responses were initially recorded under Ca $^{2+}$- and Mg $^{2+}$-free conditions, and then differing concentrations of Mg $^{2+}$ were applied by puffer pipette. Wild-type TRP channels (in *trpl*) were inhibited with an IC$_{50}$ of ~240 μm, whereas *trp*^{D621G} was ~10-fold less sensitive (IC$_{50}$ of 2.1 mm). Data (mean ± SD; $n = 4$–5 cells) fitted with a Hill equation with slope (n) of 1. The traces show responses to brief flashes (arrows) recorded first in 0 Mg $^{2+}$ (larger responses) and then in 4 mm Mg $^{2+}$, showing the greater degree of block in the *trpl* control compared with *trp*^{D621G}. *B*, Current–voltage relationships of the steady-state light-induced current obtained using continuous voltage ramps from −100 to +120 mV (duration of ramp, 1 s) in physiological Ringer's solution (in mm: 120 NaCl, 5 KCl, 1.5 CaCl$_2$, and 4 MgCl$_2$). Currents were activated by dim red light adjusted in intensity to generate approximately equal currents at resting potential (−70 mV). The traces were then corrected for leak and voltage-dependent currents by subtracting a template recorded in the dark immediately beforehand and normalized to the current at resting potential. As reported previously, the wild-type TRP channel (in the *trpl*^{302} mutant) showed dual inward and outward rectification with a low slope conductance between −10 and +40 mV primarily because of a voltage-dependent Mg $^{2+}$ block (Hardie and Mojet, 1995). In both *trp*^{D621G} and *trp*^{D621N}, the conductance was high in this region, although an additional complex double rectification developed below −40 mV and above +100 mV. Similar results were recorded from seven *trp*^{D621G} and *trp*^{D621N} cells, with essentially identical profiles being recorded in the absence of external divalent cations (data not shown). Rectification characteristics in *trp*^{D626G} appeared similar to the WT channel ($n = 4$), whereas *trp*^{D621E} was intermediate (data not shown). *C*, Block by La $^{3+}$ and RR. The degree of block (5- to 10-fold) by 1 μm La $^{3+}$ applied by puffer pipette was similar in *trpl*, *trp*^{D621G}, *trp*^{D621N}, and *trp*^{D626G}. RR at 1 μm blocked responses in *trpl* by more than fivefold, but responses in *trp*^{D621G} and *trp*^{D621N} were barely affected; an intermediate block was seen in *trp*^{D621E}. Data plotted as maximum LIC during block, normalized to response before application (mean ± SD; $n = 3$–6 cells per data point; ***$p < 0.005$ compared with *trpl* control).

20 ms in duration (half-width); however, in the absence of external Ca^{2+}, they are reduced in amplitude to <1 pA and greatly increased in duration (Henderson et al., 2000). The combination of reduced single-channel conductance, together with the lack of Ca^{2+}-dependent positive feedback, meant that quantum bumps could not be resolved in either *trp*^{D621G} or *trp*^{D621N} flies. An estimate of the single-photon response amplitude was derived instead by dividing the amplitude of responses to brighter flashes by the number of effectively absorbed photons (based on calibrations in wild-type photoreceptors), yielding values of 0.05 ± 0.02 pA ($n = 7$) in *trp*^{D621G} and 0.03 ± 0.02 pA ($n = 6$) in *trp*^{D621N}. These values, which are more than 100× smaller than the wild-type quantum bump, are an order of magnitude smaller than would have been predicted on the basis of the estimated reduction in single-channel conductance alone, consistent with the additional effect of the lack of positive feedback by Ca^{2+} influx. In contrast, quantum bumps were clearly resolved in *trp*^{D621E} flies with similar waveform to wild-type bumps. Their amplitude
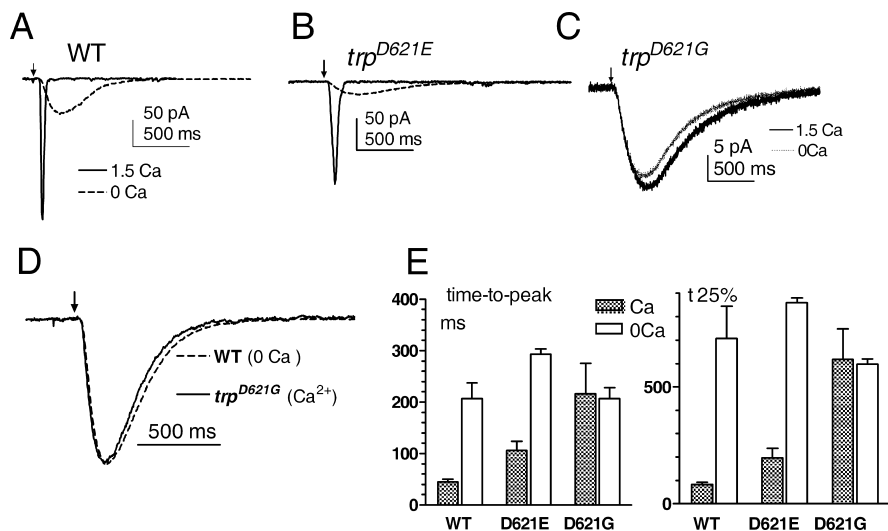
Figure 7. Loss of Ca^{2+} dependence of the LIC in Asp^{621} mutants. **A, B,** In wild-type (*trpl*) (**A**) and *trp*^{D621E} (**B**), responses to brief (1 ms) flashes in normal bath (1.5 mm Ca^{2+}) activated and deactivated rapidly. During perfusion with a Ca^{2+}-free solution, responses were reduced in amplitude and both on- and off-kinetics greatly slowed. **C,** In *trp*^{D621G}, responses were slow under both conditions and showed virtually no differences in amplitude or kinetics. **D,** Normalized, averaged responses from wild-type photoreceptors recorded in Ca^{2+}-free solution and *trp*^{D621G} recorded in the presence of 1.5 mm Ca^{2+} were indistinguishable. **E,** Summary of kinetics data: time-to-peak and time-to-decay to 25% of peak response (*t25%*). In wild-type and *trp*^{D621E} flies, both time-to-peak and time-to-decay to 25% of peak response slowed substantially in Ca^{2+}-free solution. In *trp*^{D621G}, there was no significant dependence on extracellular Ca^{2+}, and response kinetics were statistically indistinguishable from wild type.

(3.7 ± 1.1 pA; $n = 4$ cells) was ~40% of values in *trpl* or wild-type flies, now fully consistent with the estimated twofold to threefold reduction in single-channel conductance (Fig. 5*C*).

Point mutations of Asp^{621} mimic the original null *trp* phenotype

TRP channels are so-called because, during maintained bright light, the light response in *trp* mutants is transient and decays to baseline. The cause of this has long been debated and variously attributed to exhaustion of intracellular Ca^{2+} stores (Hardie and Minke, 1992; Cook and Minke, 1999) or Ca^{2+}-dependent inactivation of the residual TRPL channels (Scott et al., 1997). More recently, we showed that the decay was strictly correlated with a complete loss of PIP$_2$ during continuous illumination in *trp* mutants. We proposed that Ca^{2+} influx via TRP channels was required to inhibit PLC and that, when this influx was compromised, the maintained PLC activity resulted in hydrolysis of essentially all of the available PIP$_2$ in the microvilli (Hardie et al., 2001). We therefore asked whether eliminating Ca^{2+} influx via point mutations in the selectivity filter would also result in a *trp*-like response decay. Indeed, in flies expressing either TRP^{D621G} or TRP^{D621N}, with or without wild-type TRPL channels, responses to maintained illumination rapidly decayed to baseline, thereby mimicking the *trp* null phenotype (Fig. 8). In contrast, responses in *trp*^{D621E} failed to show this decay. To confirm that the decay in *trp*^{D621G} and *trp*^{D621N} was also associated with a loss of PIP$_2$, we monitored PIP$_2$ levels in the rhabdomeres using a PIP$_2$ biosensor, namely the PIP$_2$-sensitive ion channel Kir2.1^{R228Q}, genetically targeted to the microvillar membrane as described previously (Hardie et al., 2001, 2004). The Kir2.1 channels mediate a large constitutive inward K$^+$ current that is maintained by endogenous levels of PIP$_2$ and that is normally resistant to bright stimulation. When Kir2.1 channels were expressed in *trp*^{D621G} or *trp*^{D621N} flies, the same intensities that induced the response decay also induced the virtually complete suppression

of the Kir2.1 current over a similar time course (Fig. 8*E*), confirming the loss of PIP$_2$ reported previously in null *trp* mutants (Hardie et al., 2001). In contrast, in *trp*^{D621E}, even 10-fold brighter intensities only caused a modest (~25%) reduction in the Kir2.1 current, as reported previously for wild-type flies. This strongly suggests that it is Ca^{2+} influx, and not some other function of the TRP channel, that is essential for inhibition of PLC activity and maintaining the light response.

Asp^{621} substitutions induce retinal degeneration

It has long been known that *trp* mutants undergo light-dependent retinal degeneration. Recently, retinal degeneration in *trp* was shown to be partially rescued by an additional mutation of the Na$^+$/Ca^{2+} exchanger, CalX, suggesting that reduced Ca^{2+} influx was responsible for the retinal degeneration (Wang et al., 2005). We therefore asked whether elimination of Ca^{2+} permeation in Asp^{621} mutants was sufficient to result in retinal degeneration. In the first instance, we examined the DPP in white-eyed flies to monitor the integrity of the retina (Franceschini and Kirschfeld, 1971). In flies reared in the dark, the DPP remained clearly visible over a period of at least 3 weeks. However, in flies reared on a 12 h light/dark cycle, the DPP disappeared in 100% of *trp*^{D621N} flies within 7 d, even faster than null *trp* mutants reared under the same conditions, indicating that the retina had undergone rapid light-dependent degeneration. Similar results were obtained in *trp*^{D621G}, but, in *trp*^{D621E} flies, which have substantial remaining Ca^{2+} permeability, the DPP was still clearly visible after 2 weeks of light/dark rearing under the same conditions (Fig. 9*A*).

To confirm the degeneration, we examined retinas of dark- and light-reared *trp*^{D621N} flies by transmission electron microscopy (Fig. 9*B*). After 7 d in a 12 h light/dark cycle, profound signs of degeneration were obvious in all *trp*^{D621N} ommatidia, with most rhabdomeres either entirely absent or exhibiting extensive signs of disruption, fragmentation, and/or internalization of the microvillar structure. The cell bodies also contained multivesicular bodies and exhibited signs of phagocytosis by the surrounding pigmented glia. These morphological features were similar but more advanced than those found in *trp* null mutants reared under the same conditions (Wang et al., 2005). In contrast, the rhabdomeric structure in *trp*^{D621E} was essentially intact after 7 d light/dark rearing. Even dark-reared *trp*^{D621N} showed some abnormalities after 7 d, namely a reduced microvillar length resulting in an elongated cross-sectional profile. This was not explored further but may indicate the onset of a much slower light-independent degeneration attributable to the chronically low Ca^{2+} levels expected in these cells.

Discussion
Identification of the TRP selectivity filter
We have shown that mutating a single negatively charged residue (Asp^{621}) in the putative pore region of the prototypical TRP channel profoundly altered the permeation properties of the native conductance *in vivo*. Neutralization of Asp^{621} virtually elim-

inated permeability to Ca^{2+}, reduced single-channel conductance, altered the rectification characteristics, and alleviated channel block by Mg^{2+} and RR. Overall, a continuous trend in relative permeability to both Ca^{2+} and Na^{+} was seen as the charge on Asp^{621} was reduced, whereas increasing the side chain length by mutating Asp^{621} to glutamate significantly reduced the pore diameter An equivalent mutation in the only other acidic residue in the putative pore region (Asp^{626}) had, at most, minor effects on the biophysical properties of the pore. These results provide compelling evidence that Asp^{621} is a critical pore lining residue, required for the high selectivity for Ca^{2+}.

Previous studies have failed to identify the pore in any of the TRPC channels (for review, see Owsianik et al., 2006). The close homology of the pore regions of the *Drosophila* and vertebrate TRPC channels now allows one to suggest some structural principles for the TRPC subfamily as a whole. Assuming overall structural similarity to the bacterial cation channels KcsA (Doyle et al., 1998) and NaK (Shi et al., 2006), the pore itself is expected to be a stretch of five amino acids, after the pore helix with a sharp turn (Fig. 10B). Both the end of the pore helix, and the transition into the putative pore region (FGL), are highly conserved among the TRPCs (Fig. 10A), suggesting that these features are essential structural elements. We suggest that the FGL motif represents the turn aligning the pore with the pore helix and may also include the first residue of the pore. In *Drosophila* TRP (dTRP), the pore helix is predicted to terminate two to four amino acids N-terminal to Asp^{621}, and the pore itself is thus likely to include five residues from (LV)**D**LV(S) (critical Asp^{621} in bold). Asp^{626} lies just outside this region, and the minor effects of the trp^{D626G} mutation might be consistent with a location
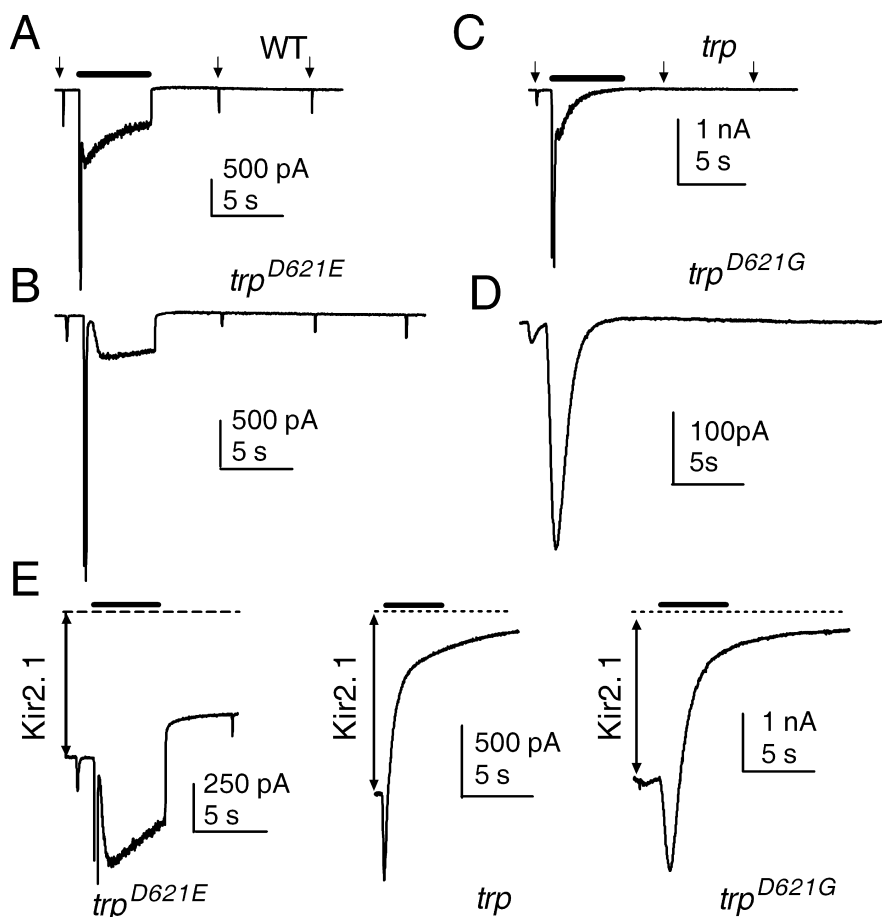

Figure 8. Eliminating Ca^{2+} permeation mimics *trp* decay. ***A***, A 5 s step of light (bar; ~3 × 10^5 photons/s) caused a rapid peak-to-plateau transition in both wild type, followed by a maintained plateau that terminated at lights off. Responses to subsequent brief test flashes (arrows) were only slightly attenuated because of light adaptation. ***B***, A similar behavior was seen in trp^{D621E}. ***C***, In a null *trp* mutant, even an ~10-fold weaker stimulus (4 × 10^4 photons/s) resulted in decay to baseline, and responses to subsequent test flashes were eliminated. ***D***, This phenotype was mimicked in trp^{D621G}. A similar behavior was also always seen in trp^{D621N} and trp^{D621G} flies with TRPL channels present (data not shown). ***E***, Responses from trp^{D621E}, *trp*, and trp^{D621G} expressing the PIP$_2$ biosensor channel Kir2.1^{R228Q}. These channels generate a large constitutive inward K$^+$ current (extent indicated by double arrow; dotted line represents zero current), which provides a measure of PIP$_2$ in the microvilli. In trp^{D621E}, bright illumination resulted in only a modest ~25% reduction in Kir2.1 current, as reported previously in wild-type or trpl flies (Hardie et al., 2001, 2004); however, 10-fold dimmer stimuli in *trp*, trp^{D621G}, and trp^{D621N} (n = 3; data not shown) resulted in near complete decay of the Kir2.1 current over a similar time course to the decay of the LIC, reflecting almost complete depletion of PIP$_2$ from the microvilli. Representative traces of at least three cells for each genotype.

in the outer vestibule of the pore. This proposed pore sequence is not conserved among the TRPC family as a whole, but the equivalent residues are well conserved in specific subgroups of the family. Thus, the sequence becomes (MV)**G**LD(D) in dTRPL, (LS)**E**VX(S) in TRPC3/6/7, and (LI)**N**LY(V) in TRPC4/5 (Fig. 10A), whereas the more divergent TRPC1 and TRPC2 have their own specific sequences (supplemental Fig. S2, available at www.jneurosci.org as supplemental material).

Interestingly, TRPL has a glycine (Gly^{628}) in the equivalent position to Asp^{621} yet still has substantial permeability to Ca^{2+} (Reuss et al., 1997). We speculate that one or other of the aspartates (Asp^{630} and Asp^{631}) in the putative TRPL pore may contribute to its Ca^{2+} permeability. TRPC3 and TRPC6 have reported P$_{Ca}$:P$_{Na}$ values of between 1.6:1 and 5:1 (Dietrich et al., 2005), perhaps consistent with our finding that the D621E substitution in dTRP preserves a modest Ca^{2+} selectivity. In TRPC4/5, Asp^{621} is substituted for asparagine, and the putative pore

sequence contains no acidic residues. This may be consistent with most recent studies of TRPC4/5 channels, which suggest that they have no specific selectivity for Ca^{2+} (P$_{Na}$:P$_{Cs}$ of ~1.0) (Plant and Schaefer, 2003).

This overall topology of the pore region is similar to that of the bacterial KcsA and NaK channels (Fig. 10) and also TRPV6 (supplemental Fig. 2, available at www.jneurosci.org as supplemental material), in which an acidic residue (Asp^{542}) has been similarly implicated as the Ca^{2+} selectivity filter (Nilius et al., 2001; Voets et al., 2004). We exploited this similarity to generate a hypothetical, minimum energy model of the dTRP pore region based on the crystal structure of KcsA (Fig. 10B). The model assumes that the pore helix ends at Gly^{618}, placing Asp^{621} in the middle of the pore (LV**D**LV). Because of the low sequence homology between dTRP and KcsA, the model should be treated with caution but serves to illustrate the structural principles discussed above. Ca^{2+} selectivity in several other channels is believed to be conferred by
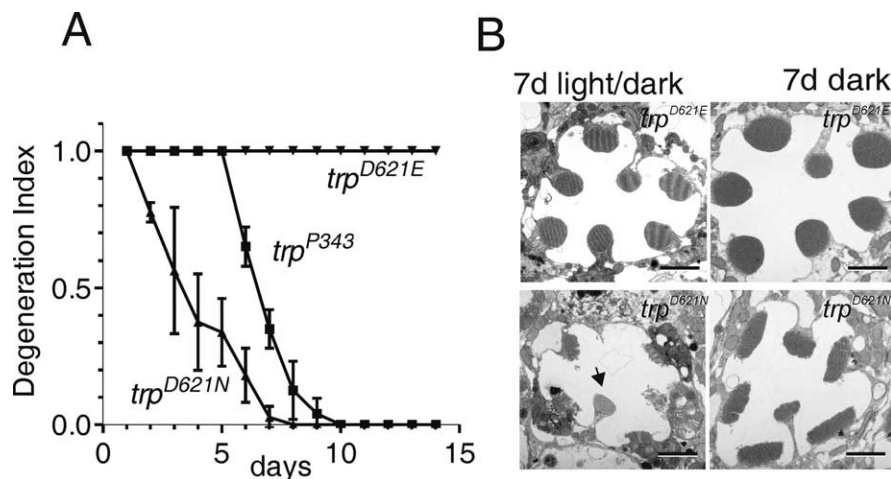
Figure 9. Retinal degeneration attributable to disruption of Ca^{2+} selectivity. **A**, Time course of degeneration monitored using the DPP. Flies were scored as having normal DPP (1.0), a weakly visible DPP (0.5), or no visible DPP (0) and a normalized degeneration index (± nominal SD) generated from cohorts of flies (n ≥ 15 for each condition). The DPP remained clearly visible in all trp^{D621E} flies even after 2 weeks and also in trp^{D621N} flies reared in the dark. However, when light reared under a 12 h light/dark cycle, the DPP in trp^{D621N} flies deteriorated even more rapidly than in trp^{P343} null mutants. **B**, Representative electron micrographs of trp^{D621E} and trp^{D621N} after 7 d of light/dark rearing and after 7 d in the dark. Light/dark-reared trp^{D621N} flies showed clear signs of degeneration in all R1–R6 photoreceptors, although the ultraviolet-sensitive R7 cell was unaffected (arrow). Scale bars, 2 μm.

a ring of four acidic residues forming a binding site for divalent ions (Yang et al., 1993; Eismann et al., 1994; Nilius et al., 2001). If, as seems likely, TRP forms a homotetramer (Reuss et al., 1997; Xu et al., 1997), Asp^{621} could be well situated to perform a similar role in dTRP.

In vivo demonstration of TRP identity

Two previous studies examined the biophysical properties of channels in cells heterologously expressing dTRP cDNAs. The first study, in insect Sf9 cells, reported permeation by divalent ions but with significantly lower Ca^{2+} permeability and much lower Ba^{2+} and Mg^{2+} permeability than for the native channel (Vaca et al., 1994). Xu et al. (1997) reported properties of channels in HEK293T cells, which, although broadly similar, again had a lower Ca^{2+} selectivity (P$_{Ca}$:P$_{Na}$ of 10:1) than that of the native TRP conductance (>50:1) and were also much less sensitive to block by La^{3+}. Although dTRP is the defining member of the TRP superfamily, these discrepancies thus raise questions about the identity of TRP as a pore-forming channel subunit in vivo.

It is generally accepted that the unequivocal identification of a pore-forming channel subunit in vivo requires the demonstration that targeted mutations in the putative pore affect the permeation properties of the channel. The list of pore properties systematically affected by mutating Asp^{621} now provides this rigorous demonstration. Although similar effects on permeation have been reported after mutagenesis of pore residues in members of the TRPV and TRPM subfamilies when heterologously expressed (for review, see Owsianik et al., 2006), to our knowledge, such a demonstration has not been achieved for any member of the TRP family in a native system and indeed has rarely been achieved for any channel.

Roles of Ca^{2+} influx

trp mutants exhibit a number of phenotypes that have been interpreted as attributable to defects in the Ca^{2+} influx. However,

TRP is not only the dominant light-sensitive channel (Reuss et al., 1997) but also has other roles. For example, TRP is coordinated into a multimolecular assembly, the signalplex, with PLC and other signaling proteins via the INAD scaffolding protein, and is required for the stability and retention of INAD in the rhabdomeres (Huber et al., 1996; Shieh and Zhu, 1996; Chevesich et al., 1997; Tsunoda et al., 1997, 2001; Xu et al., 1998; Wes et al., 1999; Li and Montell, 2000; Tsunoda et al.).

In this respect, Asp^{621} mutants, in which Ca^{2+} permeation is essentially eliminated, provide a powerful tool for testing the role of Ca^{2+} influx. Previous studies have shown that the rapid kinetics of phototransduction are dependent on external Ca^{2+}, whereas bump amplitudes are reduced and bump duration greatly prolonged in Ca^{2+}-free solutions. This has led to a model of sequential positive and negative feedback by Ca^{2+} influx acting at the level of quantum bumps (Henderson et al., 2000; Hardie and Raghu, 2001). Our results strongly support this model by showing that the response kinetics are greatly slowed and quantum bump amplitude dramatically reduced by point mutations eliminating Ca^{2+} permeation (Figs. 5, 7). Neutralizing Asp^{621} also mimicked the original trp phenotype, namely the decay of the light response during maintained illumination and the associated loss of PIP$_2$. This provides strong independent support for the proposal that the decay represents the failure of Ca^{2+}-dependent feedback acting to inhibit PLC activity rather than any other function of the TRP channel (Hardie et al., 2001).

Finally, we showed that Asp^{621} mutants underwent severe light-dependent retinal degeneration. This supports and extends the results of a recent study of a novel trp allele, trp^{14}, which expresses normal levels of TRP protein and also interacts normally with INAD (Wang et al., 2005). Despite this, trp^{14} mutants have a defective light response and undergo retinal degeneration in a similar manner to null trp mutants, suggesting that a defect in the TRP channel function, rather than its scaffolding role in the INAD complex, was responsible for the retinal degeneration (Wang et al., 2005). However, the mutation in trp^{14} was outside the pore region, and the biophysical nature of the underlying defect is not known. In contrast, we clearly show here that a point mutation specifically disrupting Ca^{2+} permeation induces light-dependent retinal degeneration, thereby providing strong additional evidence that disruption of Ca^{2+} influx leads to retinal degeneration.

In conclusion, our results provide compelling evidence that Asp^{621} is a key residue lining the pore of the prototypical TRP channel and is required for its high Ca^{2+} selectivity. The results also identify the likely location of the pore in mammalian TRPC channels and raise the possibility that the equivalent acidic residues in TRPC3, TRPC6, and TRPC7 (Glu^{686}, Glu^{618}, and Glu^{632}, respectively) may play a similar role in controlling Ca^{2+} selectivity. In addition, by generating mutants of Asp^{621} in which Ca^{2+} permeation is effectively eliminated, we have provided a direct demonstration of the essential roles of Ca^{2+} influx in many aspects of phototransduction and cell survival. Finally, the results
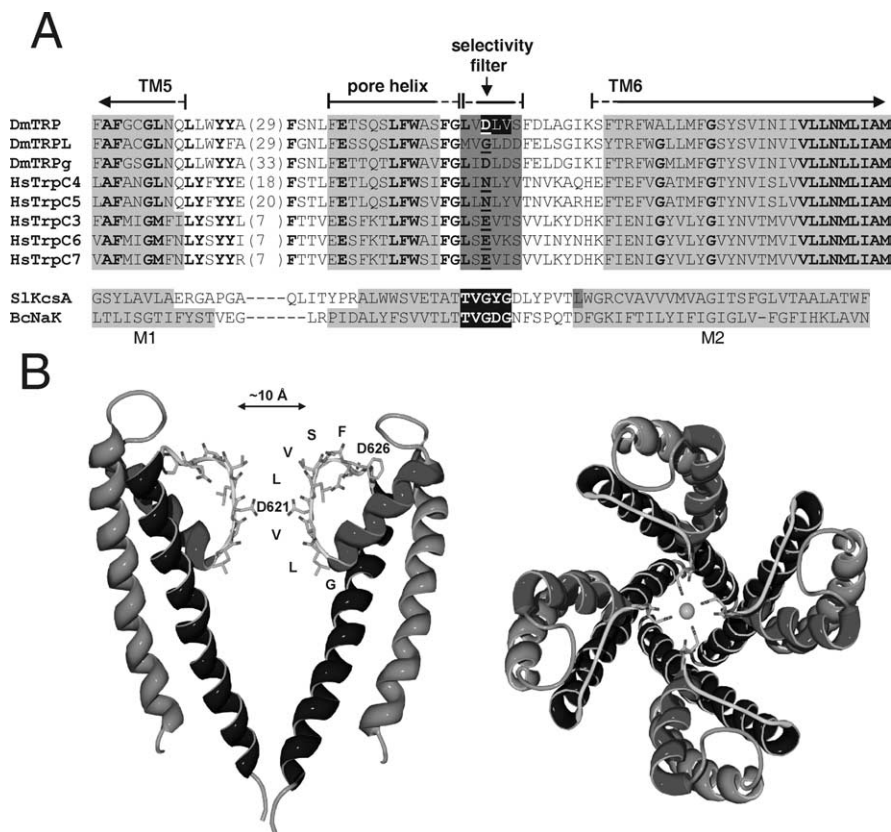
Figure 10. TRPC pore sequences and putative structure of the dTRP pore. *A*, ClustalW alignments of the TM5–TM6 region of dTRP, dTRPL, dTRPγ, mammalian TRPC3–TRPC7 (for alignments with additional TRPC and TRPV family members, see supplemental Fig. S2, available at www.jneurosci.org as supplemental material). The TM5, TM6, and pore helixes (predicted by PSIPRED) are shown in light gray (dotted lines indicate uncertainty of prediction). The pore itself is likely to be lined by five amino acids from the six residue stretch indicated in dark gray/black and includes the critical Asp⁶²¹ in dTRP and the equivalent residues N and E in other TRPCs (underlined in bold). For clarity, a variable number of amino acids (number in brackets) have been omitted from the region that links TM5 and the pore helix. The pore helix (e.g., the sequence LFW) and also the sequence leading to the selectivity filter region (FGL) are highly conserved (conserved residues in bold) among the TRPCs. Residues within the putative selectivity filter are variable although conserved within subgroups of the TRPC family (3,6,7 and 4,5). The overall topology is similar to that of the bacterial KcsA (*Streptomyces lividans*) and NaK (*Bacillus cereus*) channels (selectivity filter in black). Because of low sequence homology, ClustalW alignments of the TRPCs with KcsA and NaK are unreliable. The alignment shown is based on structural grounds (see below, *B*). *B*, Hypothetical structural model of the dTRP pore region based on the crystal structure of KcsA (1BL8). Two subunits are shown in side view on the left, and four subunits are shown from the top (extracellular) on the right. The model is based on the alignment shown in *A*, placing the critical Asp⁶²¹ in the middle of the selectivity filter (LVDLV). Models based on five different alignments, with Asp⁶²¹ ranging from the inner to outer mouth of the pore, were explored, and this gave the structure with the lowest energy. The image was generated in Swiss PDB viewer, after modeling the TRP pore region (pore helix, pore, and TM6) on the KcsA channel template. Bc, *Bacillus cereus*; Sl, *Streptomyces lividans*; Hs, *Homo sapiens*; Mm, *Mus musculus*. TRPC alignments made using ClustalW (http://www.ebi.ac.uk/clustalw/) with the PAM scoring matrix (Chenna et al., 2003). The secondary structure prediction was performed with PSIPRED (http://bioinf.cs.ucl.ac.uk/psipred/psiform.html) (McGuffin et al., 2000). Protein modeling was performed with Modeler 8.2 (Accelerys, San Diego, CA).

provide an unequivocal demonstration that the prototypical dTRP channel is a pore-forming subunit of the native light-sensitive conductance.

References

Agam K, von Campenhausen M, Levy S, Ben-Ami HC, Cook B, Kirschfeld K, Minke B (2000) Metabolic stress reversibly activates the *Drosophila* light-sensitive channels TRP and TRPL *in vivo*. J Neurosci 20:5748–5755.

Chenna R, Sugawara H, Koike T, Lopez R, Gibson TJ, Higgins DG, Thompson JD (2003) Multiple sequence alignment with the Clustal series of programs. Nucleic Acids Res 31:3497–3500.

Chevesich J, Kreuz AJ, Montell C (1997) Requirement for the PDZ domain protein, INAD, for localization of the TRP store-operated channel to a signaling complex. Neuron 18:95–105.

Cook B, Minke B (1999) TRP and calcium stores in *Drosophila* phototransduction. Cell Calcium 25:161–171.

Cosens DJ, Manning A (1969) Abnormal electroretinogram from a *Drosophila* mutant. Nature 224:285–287.

Dietrich A, Kalwa H, Rost BR, Gudermann T (2005) The diacylgylcerol-sensitive TRPC3/6/7 subfamily of cation channels: functional characterization and physiological relevance. Pflügers Arch 451:72–80.

Doyle DA, Morais Cabral J, Pfuetzner RA, Kuo A, Gulbis JM, Cohen SL, Chait BT, MacKinnon R (1998) The structure of the potassium channel: molecular basis of K⁺ conduction and selectivity. Science 280:69–77.

Dwyer TM, Adams DJ, Hille B (1980) The permeability of the endplate channel to organic cations in frog muscle. J Gen Physiol 75:469–492.

Eismann E, Muller F, Heinemann SH, Kaupp UB (1994) A single negative charge within the pore region of a cGMP-gated channel controls rectification, Ca²⁺ blockage, and ionic selectivity. Proc Natl Acad Sci USA 91:1109–1113.

Franceschini N, Kirschfeld K (1971) Etude optique *in vivo* des elements photorecepteurs dans l'oeil compose de *Drosophila*. Kybernetik 9:159–182.

Garcia-Martinez C, Morenilla-Palao C, Planells-Cases R, Merino JM, Ferrer-Montiel A (2000) Identification of an aspartic residue in the P-loop of the vanilloid receptor that modulates pore properties. J Biol Chem 275:32552–32558.

Hardie RC (1991) Whole-cell recordings of the light-induced current in *Drosophila* photoreceptors: evidence for feedback by calcium permeating the light sensitive channels. Proc R Soc Lond B Biol Sci 245:203–210.

Hardie RC (1995) Photolysis of caged Ca²⁺ facilitates and inactivates but does not directly excite light-sensitive channels in *Drosophila* photoreceptors. J Neurosci 15:889–902.

Hardie RC, Minke B (1992) The *trp* gene is essential for a light-activated Ca²⁺ channel in *Drosophila* photoreceptors. Neuron 8:643–651.

Hardie RC, Minke B (1994) Spontaneous activation of light-sensitive channels in *Drosophila* photoreceptors. J Gen Physiol 103:389–407.

Hardie RC, Mojet MH (1995) Magnesium-dependent block of the light-activated and *trp*-dependent conductance in *Drosophila* photoreceptors. J Neurophysiol 74:2590–2599.

Hardie RC, Raghu P (2001) Visual transduction in *Drosophila*. Nature 413:186–193.

Hardie RC, Raghu P, Moore S, Juusola M, Baines RA, Sweeney ST (2001) Calcium influx via TRP channels is required to maintain PIP₂ levels in *Drosophila* photoreceptors. Neuron 30:149–159.

Hardie RC, Martin F, Chyb S, Raghu P (2003) Rescue of light responses in the *Drosophila* "null" phospholipase C mutant, *norpA^P24*, by the diacylglycerol kinase mutant, *rdgA*, and by metabolic inhibition. J Biol Chem 278:18851–18858.

Hardie RC, Gu Y, Martin F, Sweeney ST, Raghu P (2004) In vivo light-induced and basal phospholipase C activity in *Drosophila* photoreceptors measured with genetically targeted phosphatidylinositol 4,5-bisphosphate-sensitive ion channels (Kir2.1). J Biol Chem 279:47773–47782.

Henderson SR, Reuss H, Hardie RC (2000) Single photon responses in *Drosophila* photoreceptors and their regulation by Ca²⁺. J Physiol (Lond) 524:179–194.

Huber A, Sander P, Gobert A, Bahner M, Hermann R, Paulsen R (1996) The transient receptor potential protein (Trp), a putative store-operated

Ca^{2+} channel essential for phosphoinositide-mediated photoreception, forms a signaling complex with NorpA, InaC and InaD. EMBO J 15:7036–7045.

Jung S, Muhle A, Schaefer M, Strotmann R, Schultz G, Plant TD (2003) Lanthanides potentiate TRPC5 currents by an action at extracellular sites close to the pore mouth. J Biol Chem 278:3562–3571.

Li HS, Montell C (2000) TRP and the PDZ Protein, INAD, form the core complex required for retention of the signalplex in *Drosophila* photoreceptor cells. J Cell Biol 150:1411–1422.

Liu X, Singh BB, Ambudkar IS (2003) TRPC1 is required for functional store-operated Ca^{2+} channels. Role of acidic amino acid residues in the S5–S6 region. J Biol Chem 278:11337–11343.

McGuffin LJ, Bryson K, Jones DT (2000) The PSIPRED protein structure prediction server. Bioinformatics 16:404–405.

Minke B, Wu C-F, Pak WL (1975) Induction of photoreceptor noise in the dark in a *Drosophila* mutant. Nature 258:84–87.

Montell C (1999) Visual transduction in *Drosophila*. Annu Rev Cell Dev Biol 15:231–268.

Montell C (2005) The TRP superfamily of cation channels. Sci STKE 2005:re3.

Montell C, Rubin GM (1989) Molecular characterization of Drosophila *trp* locus, a putative integral membrane protein required for phototransduction. Neuron 2:1313–1323.

Montell C, Jones K, Hafen E, Rubin G (1985) Rescue of the *Drosophila* phototransduction mutation *trp* by germline transformation. Science 230:1040–1043.

Niemeyer BA, Suzuki E, Scott K, Jalink K, Zuker CS (1996) The *Drosophila* light-activated conductance is composed of the two channels TRP and TRPL. Cell 85:651–659.

Nilius B, Vennekens R, Prenen J, Hoenderop JG, Droogmans G, Bindels RJ (2001) The single pore residue Asp^{542} determines Ca^{2+} permeation and Mg^{2+} block of the epithelial Ca^{2+} channel. J Biol Chem 276:1020–1025.

Obukhov AG, Nowycky MC (2005) A cytosolic residue mediates Mg^{2+} block and regulates inward current amplitude of a transient receptor potential channel. J Neurosci 25:1234–1239.

Owsianik G, Talavera K, Voets T, Nilius B (2006) Permeation and selectivity of TRP channels. Annu Rev Physiol 68:685–717.

Phillips AM, Bull A, Kelly LE (1992) Identification of a *Drosophila* gene encoding a calmodulin-binding protein with homology to the *trp* phototransduction gene. Neuron 8:631–642.

Plant TD, Schaefer M (2003) TRPC4 and TRPC5: receptor-operated Ca^{2+}-permeable nonselective cation channels. Cell Calcium 33:441–450.

Raghu P, Usher K, Jonas S, Chyb S, Polyanovsky A, Hardie RC (2000) Constitutive activity of the light-sensitive channels TRP and TRPL in the *Drosophila* diacylglycerol kinase mutant, rdgA. Neuron 26:169–179.

Ramsey IS, Delling M, Clapham DE (2006) An introduction to TRP channels. Annu Rev Physiol 68:619–647.

Ranganathan R, Harris GL, Stevens CF, Zuker CS (1991) A *Drosophila* mu-

tant defective in extracellular calcium-dependent photoreceptor deactivation and rapid desensitization. Nature 354:230–232.

Reuss H, Mojet MH, Chyb S, Hardie RC (1997) In vivo analysis of the *Drosophila* light-sensitive channels, TRP and TRPL. Neuron 19:1249–1259.

Scott K, Sun YM, Beckingham K, Zuker CS (1997) Calmodulin regulation of *Drosophila* light-activated channels and receptor function mediates termination of the light response *in vivo*. Cell 91:375–383.

Shi N, Ye S, Alam A, Chen L, Jiang Y (2006) Atomic structure of a Na^{+}- and K^{+}-conducting channel. Nature 440:570–574.

Shieh BH, Zhu MY (1996) Regulation of the TRP Ca^{2+} channel by INAD in *Drosophila* photoreceptors. Neuron 16:991–998.

Tsunoda S, Sierralta J, Sun YM, Bodner R, Suzuki E, Becker A, Socolich M, Zuker CS (1997) A multivalent PDZ-domain protein assembles signalling complexes in a G-protein-coupled cascade. Nature 388:243–249.

Tsunoda S, Sun Y, Suzuki E, Zuker C (2001) Independent anchoring and assembly mechanisms of INAD signaling complexes in *Drosophila* photoreceptors. J Neurosci 21:150–158.

Vaca L, Sinkins WG, Hu Y, Kunze DL, Schilling WP (1994) Activation of recombinant trp by thapsigargin in Sf9 insect cells. Am J Physiol 267:C1501–C1505.

Voets T, Prenen J, Vriens J, Watanabe H, Janssens A, Wissenbach U, Bodding M, Droogmans G, Nilius B (2002) Molecular determinants of permeation through the cation channel TRPV4. J Biol Chem 277:33704–33710.

Voets T, Janssens A, Droogmans G, Nilius B (2004) Outer pore architecture of a Ca^{2+}-selective TRP channel. J Biol Chem 279:15223–15230.

Wang T, Jiao Y, Montell C (2005) Dissecting independent channel and scaffolding roles of the *Drosophila* transient receptor potential channel. J Cell Biol 171:685–694.

Wes PD, Chevesich J, Jeromin A, Rosenberg C, Stetten G, Montell C (1995) TRPC1, a human homolog of a *Drosophila* store-operated channel. Proc Natl Acad Sci USA 92:9652–9656.

Wes PD, Xu XZ, Li HS, Chien F, Doberstein SK, Montell C (1999) Termination of phototransduction requires binding of the NINAC myosin III and the PDZ protein INAD. Nat Neurosci 2:447–453.

Xu XZS, Li HS, Guggino WB, Montell C (1997) Coassembly of TRP and TRPL produces a distinct store-operated conductance. Cell 89:1155–1164.

Xu XZS, Choudhury A, Li XL, Montell C (1998) Coordination of an array of signaling proteins through homo- and heteromeric interactions between PDZ domains and target proteins. J Cell Biol 142:545–555.

Yang J, Ellinor PT, Sather WA, Zhang JF, Tsien RW (1993) Molecular determinants of Ca^{2+} selectivity and ion permeation in L-type Ca^{2+} channels. Nature 366:158–161.

Yu FH, Yarov-Yarovoy V, Gutman GA, Catterall WA (2005) Overview of molecular relationships in the voltage-gated ion channel superfamily. Pharmacol Rev 57:387–395.

Zhu X, Chu PB, Peyton M, Birnbaumer L (1995) Molecular cloning of a widely expressed human homologue for the *Drosophila trp* gene. FEBS Lett 373:193–198.